Application and validation of measurement techniques related to the physical modelling of the atmospheric boundary layer in a new boundary layer wind tunnel

PROJECT ID: 127919

FINAL SCIENTIFIC REPORT

Márton Balczó, PhD

February 13, 2023

Keywords: atmospheric boundary layer, boundary layer wind tunnel, flow measurement techniques, wind loading, ventilation, tracer dispersion

1 Executive summary

In the framework of this PD project, I accomplished two major projects[1], which were both successfully finished in 2022, although after serious delays.

A) In project 'A', this PD project funded my work as technical /engineering leader of the project, assisting the leader/manager of the project, Prof Dr. János VAD.

B) In project 'B' this PD project funded my work as senior researcher, assisting the team and principial investigator Dr. Gergely KRISTÓF.

Project 'A', entitled 'Establishment of an Atmospheric Flows Laboratory' (Competitive Central Hungary Operative Programme, project ID: VEKOP 2.3.3-15-2017-00017) was an infrastructural project, running from 2017 to 2022, with a funding of 411.2 million HUF (~1.1 M EUR) aimed to construct an atmospheric boundary layer wind tunnel measuring up to international standards, together with a laboratory accommodating it, as well as to develop the corresponding measurement systems and computational background [1]. I managed the specification, design, acquisition and initial operation of the wind tunnel and measurement equipment and establishing the operational practice of the new laboratory. Project 'A' suffered a 2-year delay, cost increases due to external factors, and it was re-located twice into various buildings of the BME campus (and correspondingly, redesigned twice.) In the end, instead of a new laboratory and a new wind tunnel, the existing laboratory and wind tunnel were modified and rebuilt and equipped with state-of-the-art measurement instrumentation. As the equipment became operational in last year (2022) the measurement tasks I committed to in my original research plan, were only documented in research reports, MSc theses and not in peer-reviewed journals. One must note, that the introduction and operational readiness of new measurement techniques/equipment itself – while it required considerable effort from the author – is not the subject of journal publications. Only two local conference presentations were held on the subject [3-4]. For this reason, this report will describe the work done in project 'A' in more detail starting from Chapter 3. Project A was finished on the 31 of May, 2022, although some tasks of my original Research plan were continued until January 2023 [2].

Tasks performed in project 'A' (with timeframe of elaboration):

1.	Design of the wind tunnel lab, including a new model workshop.	2019-22
2.	Design of a new wind tunnels	2018-19
3.	Design and construction of a simultaneous pressure measurement system	2018-19
4.	Programming of the data analysis software for multi-channel pressure measurements	2019-20

[1] No personal funding was provided to me from project A, thus this PD project funded my base income and my work in this project for 3 years. From project B, I got 5 months of funding, totalling 500.000 HUF, otherwise my participation was funded from this PD project.

5. Programming of a measurement control and data acquisiton program 2018-22
6. Generation of atmospheric boundary layers in the wind tunnel 2022
7. Test measurement of wind pressures on an arched roof structure 2022-23
8. High-frequency force balance technique (HFFB) – replaced by low-frequency balance 2019

Project ‘B’, NKFIH K 124439 project 'Air quality oriented urban design strategies' was oriented towards an architectural optimization of urban settings from the air quality point of view. The validation of the newly developed CFD methodology was performed by wind tunnel tests of selected building configurations: My role was assisting the measurements. My work in project ‘B’ is well documented in a published journal paper, an international conference paper, and a recently submitted journal paper. For this reason, my work in project ‘B’ is only described shortly here.

Tasks performed in project ‘B’

I took part in the validation measurements of this project consisting of Laser-Doppler Velocimetry (LDV) and tracer gas experiments in the existing wind tunnel in various street building configurations favourable to the ventilation of the modelled urban area, to validate out comparable simulations.

The test consisted of measurement of wind field using LDV and the concentrations of a methane tracer gas using a fast flame-ionisation detector (FID) device. My role was programming the measurement data acquisition using Labview, including the Large Wind Tunnel Traversing system (see later in Chapter 7). During this extensive campaign, over 1000 individual tracer measurements were carried out for the investigated 3 configurations shown in **Figure 1**. The test campaign took several months to accomplish and took as much as 193 wind tunnel test hours.

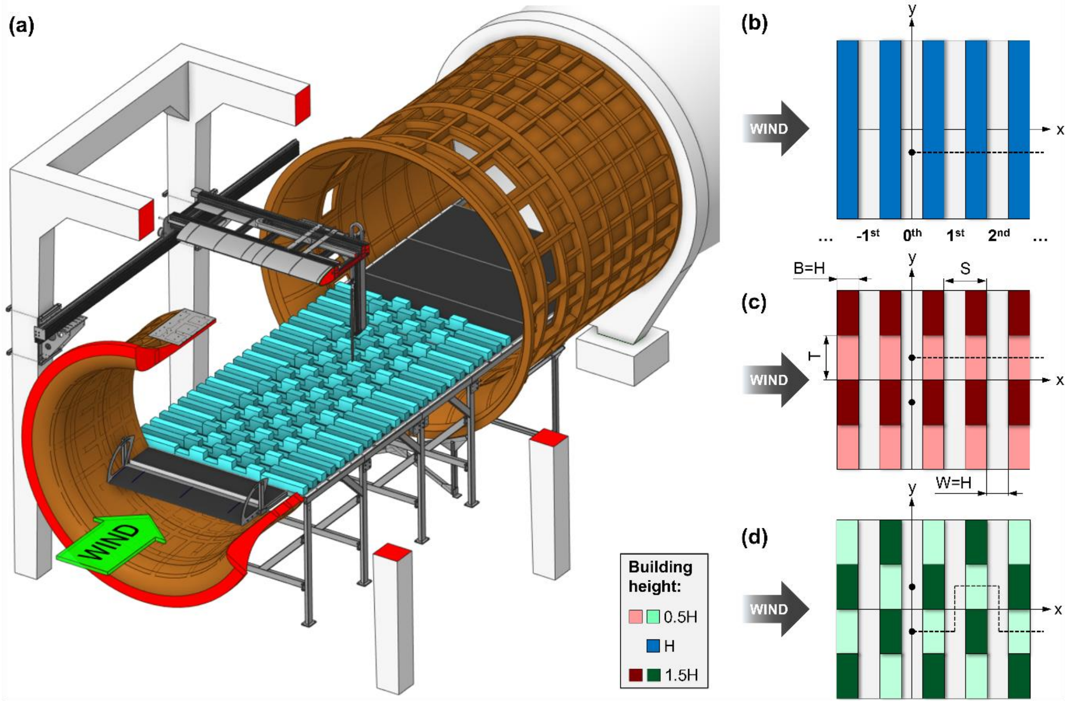

Figure. 1. Experimental setup (a) and the investigated building patterns in project ‘B’: uniform street canyons b), matrix/aligned towers c), staggered towers d). The black dots designate the tracer sources, and the dashed lines indicate the locations of the measurement points at z/H = 1.2.

The test were run successfully, and results with other project participants were published in [5-6] and publication in another journal is further pursued [7].

Overall, my post-doctoral project PD 127919 reached majority of the promised outcome: a solid operational readiness of the wind tunnel laboratory in a wide range of applications and measurement techniques in the field of building- and environmental aerodynamics: Laser-Doppler Velocimetry, High Frequency Simultaneous Pressure Measurements, Tracer dispersion measurements. These were proven in several applications and test measurements. The underlying infrastructure project with a budget of 411 million HUF, although after major changes and delays, was successfully accomplished. Tasks relating to project 'B' were all finished.

The promised outcome has not been reached or only partially reached in the following areas: introduction of High Frequency Force Balance (HFFB) measurements in wind tunnel (only low frequency balance was developed) and the publication of a peer-reviewed journal paper from outcomes of project 'A'. Instead of writing a static wind tunnel guideline, I focussed on the implementation of the techniques into operational software, serving as practical guidance for the wind tunnel staff in the daily use of the laboratory.

2 References

[1] Website of the original project proposal of Project 'A': www.bmeafl.wordpress.com

[2] Final report of Project 'A': Short Summary in English and Hungarian. https://simba.ara.bme.hu/~balczo/out/K127919/02_AFL-VEKOP_final_report.pdf

[3] Balczó, M: The role of wind tunnel testing in the determination of wind loading of buildings and engineering structures, IDEA 2019 Conference, Kecskemét, Hungary, 25-26 April, 2019., *2019 (conference without proceedings)* https://simba.ara.bme.hu/~balczo/out/K127919/03_Balczo_IDEA_2019.pdf

[4] Balczó, Márton; Fenyvesi, Bence: MÁV T típusú felsővezetéki oszlopok szélcsatorna vizsgálata. XV. Vasútvillamosítási Konferencia, Harkány, 2021. október 19-21. (*Wind tunnel test of type T catenary masts of the Hungarian State Railways. XV. Conference on Rail Electrification. 19-21.10.2021, Harkány, Hungary – in Hungarian. Conference without proceedings)* https://simba.ara.bme.hu/~balczo/out/K127919/04_T-type_catenary_pres.pdf

[5] Papp, Bálint; Kristóf, Gergely; Istók, Balázs; Koren, Márton; Balczó, Márton; Balogh, Miklós: Measurement-driven Large Eddy Simulation of dispersion in street canyons of variable building height. JOURNAL OF WIND ENGINEERING AND INDUSTRIAL AERODYNAMICS 211 Paper: 104495, 16 p. (2021) https://doi.org/10.1016/j.jweia.2020.104495

[6] Papp, Bálint; Istók, Balázs; Koren, Márton; Balczó, Márton; Kristóf, Gergely: Statistical assessment of the ventilation of street canyons based on time-resolved wind tunnel experiments. In: Jurcakova, Klara PHYSMOD 2022 - International Workshop on Physical Modeling of Flow and Dispersion Phenomena, Prága, Csehország : Ústav termomechaniky AV ČR (2022) 282 p. pp. 143-155. , 12 p. https://simba.ara.bme.hu/~balczo/out/K127919/06_Physmod2022_paper.pdf

[7] Papp, B., Istók, B., Koren, M., Balczó, Kristóf, G. (2022). Statistical assessment of the concentration fluctuations in street canyons with homogeneous and variable roof height. *submitted to Building and Environment on 15/09/2022. Review resultfrom two reviewers: Major improvement required / rejected. After incorporating reviewer comments, resubmission to other journal planned in March 2023.* https://simba.ara.bme.hu/~balczo/out/K127919/07_BAE-submission.pdf

3 Design of the wind tunnel lab, including a new model workshop

3.1 Description

As mentioned in the Executive summary, the new lab has been relocated and re-designed twice. In the following I show the second unrealized laboratory design, and the realized lab arrangement. (For the very first location, a lab and wind tunnel design was elaborated before this PD project started, thus that design is not discussed here.)

3.1.1 Goldmann building – design facilitating a new wind tunnel

The site of the first re-location was in the basement of the earlier 'Goldmann' canteen of the University called. In the design process:

1. I formulated the design requirements for all rooms of the lab, including wind tunnel dimensions and utility connections
2. Cooperated with the building services engineer in the design of the wind tunnel cooling system
3. Cooperated with the Chancellor's Office in all aspects of the design and building process

The location allowed for a large recirculation wind tunnel with 3.8 x 2.2 m test section with 20 m length, and a generous area of rooms to service the wind tunnel testing process. (See design plan in **Appendix 1**). Due to high demolition costs, non-fundable, from the funding VEKOP project, this location and lab design had to be abandoned in autumn 2019.

Table 1. Rooms of the laboratory with functions.

Name	**Area [m^2]**	**Function**
Wind tunnel space	600	space taken by the recirculating wind tunnel components
Wind tunnel cooling system	25	The cooling system of the wind tunnel was placed on the roof, but a puffer tank had to be facilitated on the ground floor.
Model workshop	106	Construction of models on 3m turntables, area for instrumentation in front of the WT test section.
Storage	110	storage of: boundary layer generators, models, model building material, optional wind tunnel elements,
Laboratory	37	workplace for 3-4 researchers and students
meeting room	28	place for clients or externeal research colleborators, space for seminar events.
Social spaces, corridors	61	
Total	**967**	price estimate, summer 2019: 100 million HUF (demolition) + 170 million HUF (construction)

3.1.2 AE building – existing wind tunnel lab redesign

After abandoning the plans shown previously, in agreement with the Funding Authority, it has been decided that no new wind tunnel will be built, but the laboratory of the existing 2.6 m-test section wind tunnel will be reshaped and adapted to host state-of the art instrumentation including a time-resolved PIV system. Several rooms have been repurposed. Construction on a total of 572 m^2 area took place between October 2020 and January 2021. (See design plan in **Appendix 2** and in **Table 2.**)

3.1.3 Design of a model and prototype workshop

After that, my work focussed on equipping the model and prototype workshop, which took me 1.5 years including selection/specification of the most necessary machines and tools, managing their lengthy acquisition, and designing their functional arrangement in the highly limited space of only 60 m^2. (See realized workshop in **Appendix 3**.)

Table 2. Rooms with new functions in the existing wind tunnel laboratory (Building AE).

Name	Area [m^2]	Function / measures
Wind tunnel test section / measurement room	292	New flooring, new windows, new crane to lift interchangeable test section elements and models into the test section.
Wind tunnel electrical rooms	71	rebuild of ÉL building low-voltage power distribution to supply AE building and wind tunnel. New 400V power supply cable for wind tunnel.
Laser optical lab	35	Space for setup calibration and eventual test measurement of the PIV and LDV systems. Instrument storage.
Model workshop	60	Construction of models on 2.5 m turntables. Manufacture of models, and prototypes, with various technologies. New concrete and epoxy flooring, ne windows
Storage	74	storage of: boundary layer generators, models, model building material, optional wind tunnel elements,
Laboratory, guest researcher room	25	workplace for 2 researchers, workplace for 1 visiting scientist.
other spaces	19	
Total	**578**	contracted price, autumn 2020: 5 million HUF (demolition) + 133 million HUF (construction)

Table 3. Model workshop equipment, selected, specified by the Author

Name	value [1000 HUF]	Manufacturer, type	other specifics and purpose
conventional milling and drilling machine	2400	Optimum MP4-P	with digital redout | for milling of metal and plastic model parts & components
drill press	*- (existing)*		
motorized sheet metal shear	*- (existing)*		*up to 3 mm mild steel, 1.25m cutting length |*
welding table and clamping set	~2900	Siegmund Professional 750 with 16 mm claming system	for welding and positioning/assembly of models | 1.5 x 1 x 0.1 m with 50 x 50 mm grid of 16 mm diamtere holes
metal band saw	172		
scrollsaw	700	Hegner Multicut	precision sawing of steel, aluminium plastics and wooden parts
3D printer	771	Qidi-tech i-Fast	FDM type, dual extruder, 330 x 250 x 320mm, heated chamber
grinder with sanding belt	111	Holzmann DSM 100200B	sanding, deburring
polishing machine	228	Holzmann DSM 200	with 3M deburring wheels
electric hand tools	~300	various	circle saw, hand drill, etc. for works with wood and plastics.
various handtools and furniture	~ 2000	various	workshop cupboards, shelves, material storage racks, tables, vices, hand tools, soldering equipment, sheet meal tools, vacuum cleaner
Total	**~9582**		
Outstanding machines			
lathe	*~1200*	*Optimum TU 2506*	*(planned) manufacturing of cylindrical parts, e.g., pressure probes, pressure taps, connectors.*
mixed mode laser cutter	*16 000*	*HSG Laser SD-LASER PRO 1325M 280W*	*(planned) cutting of mild steel and acrylic parts*

3.2 Outcome

A fully operational wind tunnel laboratory with the necessary storage, experiment preparation and model manufacturing capabilities. Example of a manufactured wind tunnel model (3D printed, assembly and pressure tapping performed in the new model workshop under supervision of the Author) is shown in **Fig. 2.**

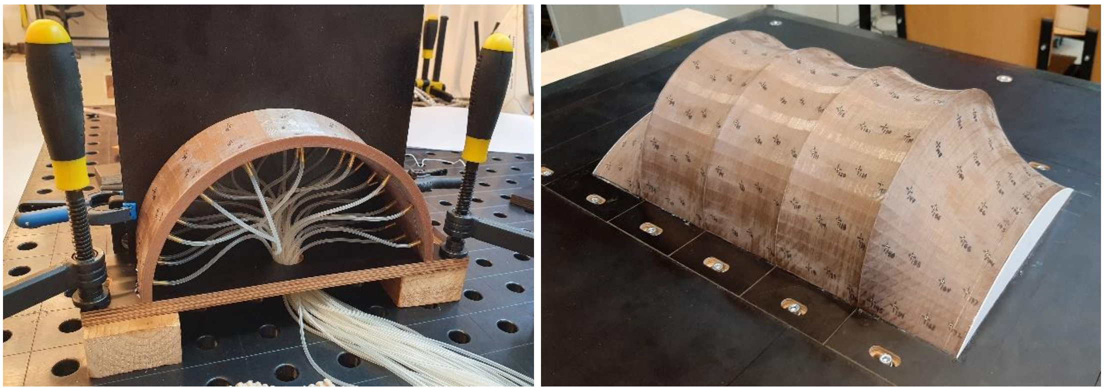

Figure 2. Modular model of an arched roof with 180 pressure taps, manufactured in the workshop

3.3 Acknowledgement of contributors

- Norman Mérnöki Iroda Kft. (Norman Engineering Bureau Ltd.): Architectural design of laboratory in Goldmann Building
- Pálinkás, József: Architectural design of laboratory renovation in building AE.
- BME Chancellory: tendering, contracting and technical inspection of construction works, administration of workshop tool/machine acquisitions.
- Krisztián Hincz, PhD, associate professor (BME Faculty of Civil Engineering, Department of Structural Mechanics), Shirly Pool Blanco MSc, PhD student: Arched roof model shown in Figure 1.

3.4 References

[8] Norman Engineering Office Ltd.: Budapest University of Technology and Economics, Goldmann Building, Atmospheric Flow Laboratory - Construction Plan, 31 May, 2019. *(In Hungarian)*
https://simba.ara.bme.hu/~balczo/out/K127919/08_Goldmann_laboratorium_kiviteli_terv.pdf
(see also Appendix 1.)

4 Design of a new wind tunnels

4.1 Description

4.1.1 A closed return boundary-layer wind tunnel for the Goldmann building

Envisaged in the original research plan of this PD project, I prepared the geometric and aerodynamic design of a boundary-layer wind tunnel. Due to the relocation of the project to Goldmann building, this wind tunnel had to be adapted to the constraints of that site. The design itself included the following tasks:

- Determination of wind tunnel type and layout, main dimensions, cross sections
- Pressure loss and power calculations based on literature data. Selection of wind tunnel fans
- Determining other requirements, servicing, ventilation etc. of the wind tunnel
- Determination of the main parameters/requirements of the wind tunnel cooling system

Main parameters are shown in **Table 4**., the layout in **Figure 3**, the power calculation in **Appendix 4.** The design did not contain the structural design/construction of the individual wind tunnel elements. All tasks were performed by myself, except the acoustic design (e.g. specification of noise separating walls), the design of structural installation of the fans, and the cooling system design, which were performed by the acoustics and the building services subcontractors in my coordination.

Table 4. Closed return boundary-layer wind tunnel parameters

Type	closed return, horizontal with adjustable roof, with cooling system.
External dimensions	37 x 15 x 5 m
Test section size	3.8 x 2.1-2.6 x 18 m
Flow length along centre line	77 m
Contraction ratio	3
Max. velocity in test section	26 m/s
Total pressure loss (including test section models)	696 Pa
Power requirement	206 kW
Fan type	6 off-the-shelf fans with silencers in 3 x 2 parallel arrangement Helios G-8, D=1250 mm, 34 kW, 1480 rpm
Cooling system	
Estimated structural mass (steel)	~80 t
Price estimate, summer 2019	232 million HUF

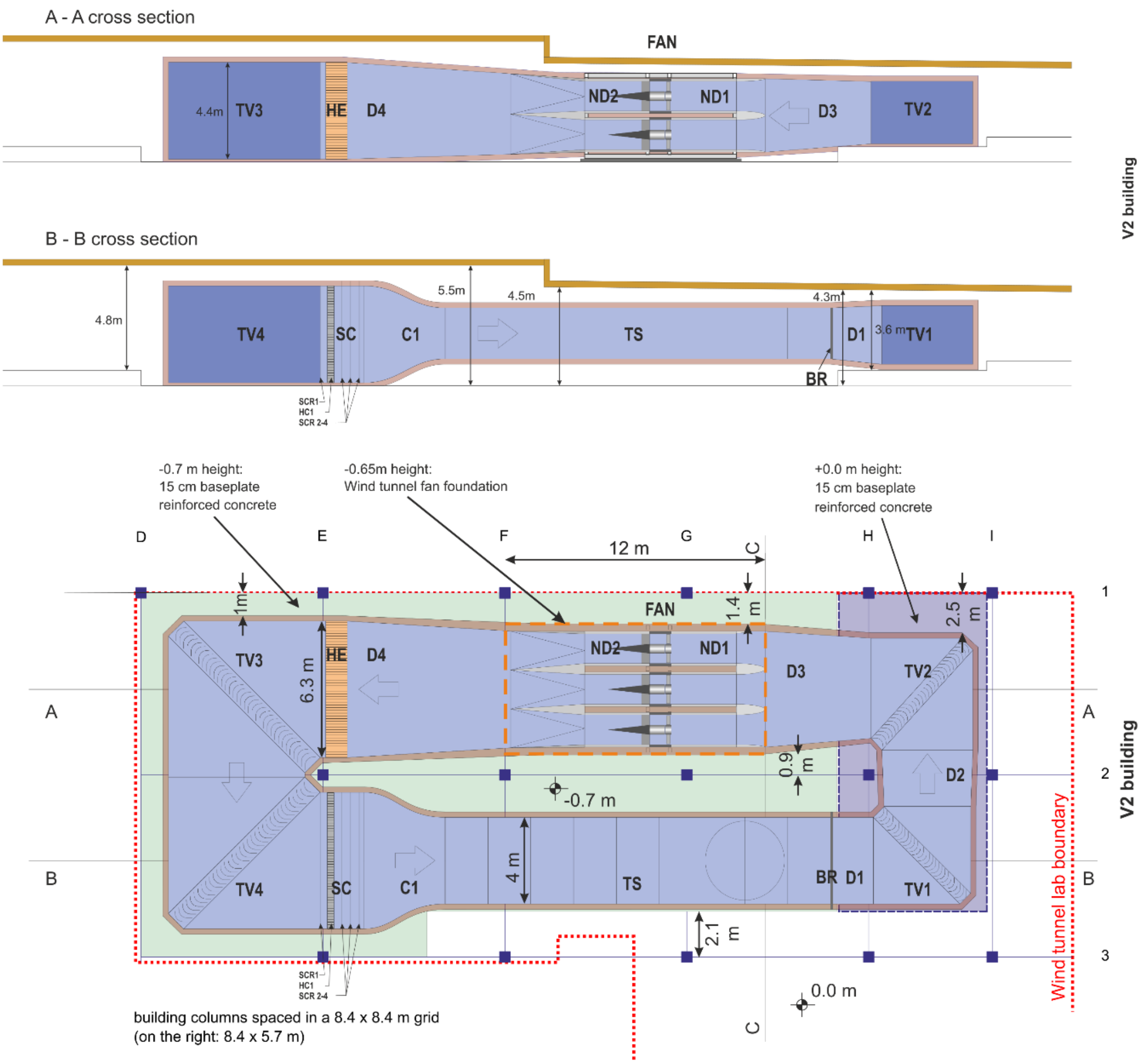

Figure 3. Plan and elevation view of the closed return wind tunnel designed by the Author (TS: Test section, BR: Breather, D1-4:diffusers, TV1-4: Turning vanes, HE: heat exchanger, SCR1-4: screens, HC1: honeycomb flow straightener, TS: test section, C1: Contraction)

4.1.2 Upgrade of the existing wind tunnel in the AE building

After the Goldmann site had to be abandoned, I dealt with the design tasks of the upgrade of the existing closed-return, open-test section wind tunnel. These tasks can be considered minor, in comparison to the design of a new wind tunnel and included: specification of a new mobile crane for lifting heavy models of up to 200 kg into the wind tunnel, installation of test section ladders.

4.2 Outcome

The design of a large closed-return boundary layer wind tunnel has been prepared, although not built, is available and can be used in the future after adaptation to requirements of the specific site.

4.3 Acknowledgement of contributors

- Gábor Koscsó, hon. associate professor, Hangmérnök Ltd.: acoustic design: design of noise abatement measures) and design of the fan installation
- Szilágyi Sándor, Komfort 2001 Building Services Design Ltd.: - Cooling system design

4.4 References

[9] Balczó, Márton: Technical description of the atmospheric boundary layer wind *tunnel (Az atmoszférikus határréteg szélcsatorna technológiai leírása)* version 1.6, 01/08/2019 *(In Hungarian and German)* https://simba.ara.bme.hu/~balczo/out/K127919/09_Wind_tunnel%20_docs_GE_HU.pdf

[10] Hangmérnök Ltd.: Aerodynamic and acoustic plan for an atmospheric boundary layer wind tunnel (*Légtechnikai és akusztikai terv atmoszférikus határréteg szélcsatorna felépítéséhez)* 30/01/2020 *(In Hungarian)* https://simba.ara.bme.hu/~balczo/out/K127919/10_Akusztikai_dokumentacio.pdf

[11] Komfort 2001 Building Services Design Ltd.: Documentation to the engineering design contract "Atmospheric Flows Laboratory" wind tunnel of the Budapest university of technology and Economics (*Budapesti Műszaki Egyetem Goldmann épületébe telepítendő „Atmoszférikus Áramlások Laboratórium" szélcsatorna gépészeti tervezéséről szóló szerződés elszámolási dokumentációja)* 30/01/2020 *(In Hungarian)* https://simba.ara.bme.hu/~balczo/out/K127919/11_Komfort_2001_dokumentacio.pdf

5 Design and construction of a high-frequency simultaneous pressure measurement system

5.1 Description

Pressure distribution measurement in wind tunnels were traditionally performed using mechanical multiplexing (i. e. connecting pressure taps to a single sensor each after each), demanding extreme long measurement times (e.g. in case of 400 pressure taps: 400 x 1 minute, more than 6 hours) and lacking information about the temporal correlation between measurement locations.

Simultaneous measurement of pressures using multiple sensors (one for each tap) on surfaces of a building of structure makes the determination of the instantaneous wind loads on any structure possible, assuming that the surface is simple enough to be equipped with pressure taps, and pressure distribution can thus be integrated along the surface. With the exemption of lattice or porous structures, and buildings with highly structured façade elements, many buildings and structures fit that condition. However, the number of pressure taps required can go into the hundreds, depending on building size and complexity. Such custom-built pressure measurement systems are in use in some laboratories since the 1990's and are also available commercially from few vendors globally, however at high prices. The limited funding available from Project 'A' required thus a self-made system, based on low-cost pressure sensors available on the market (~40 to 50 EUR unit price).

We designed and constructed a modular and expandable system, consisting of 40 pieces of 10-sensor units, so called satellite units (giving a total of 400 channels). The low channel count satellite units allow for using different and shorter pressure tubing lengths, placing sensors closer to pressure taps and inside smaller models as compared to commercially available systems which have high channel-count modules (32, 64 or 128). Data acquisition is analogue, through a high-channel-count data acquisition system, and a LabVIEW based PC application. Most important parameters of our system, pictured in **Figure 4** is shown in **Table 5.**

Table 5. Parameters of the designed multi-channel pressure measurement system

Sensor type	Honeywell Trustability HSC, HSCDRRN002NDAA5, with temperature compensated, amplified output, 12 bit
Range	+/- 500 Pa differential
Sensor pressure tubing	ID1.2 mm, OD, 1.8 mm PTFE (0.5…1 m tubelength between sensor and model pressure tap)
Temporal resolution od sensors	1 ms
Compensated pressure fluctuation frequency	400-500 Hz (depending on tube length)
Accuracy (incl. non-linearity, pressure hysteresis, and non-repeatability.)	0.25% full scale (+/- 2.5 Pa)
DAQ system	National Instruments PXI 1062Q chassis with PXIe-8133 controller
DAQ card	5 pcs of NI 6225 80-channel, 250kS/s A/D card, synchronized through PXI bus
Sampling frequency (max.)	3125 Hz (on each channel)
cabling	2 pcs of 10 m NI-SHC-68-68-EPM shielded analogue cables between each DAQ card and a signal distributor box.
Layout	5 signal distribution boxes, 8 satellite units connecting to each signal distributor box through flat cables, 10 sensors in each satellite unit.
Sensors, boxes, cabling, cost	6 million HUF (15 000 HUF/channel)
DAQ system cost*	11 million HUF (27 000 HUF/channel)

**DAQ system cost can be reduced by choosing another DAQ platform.*

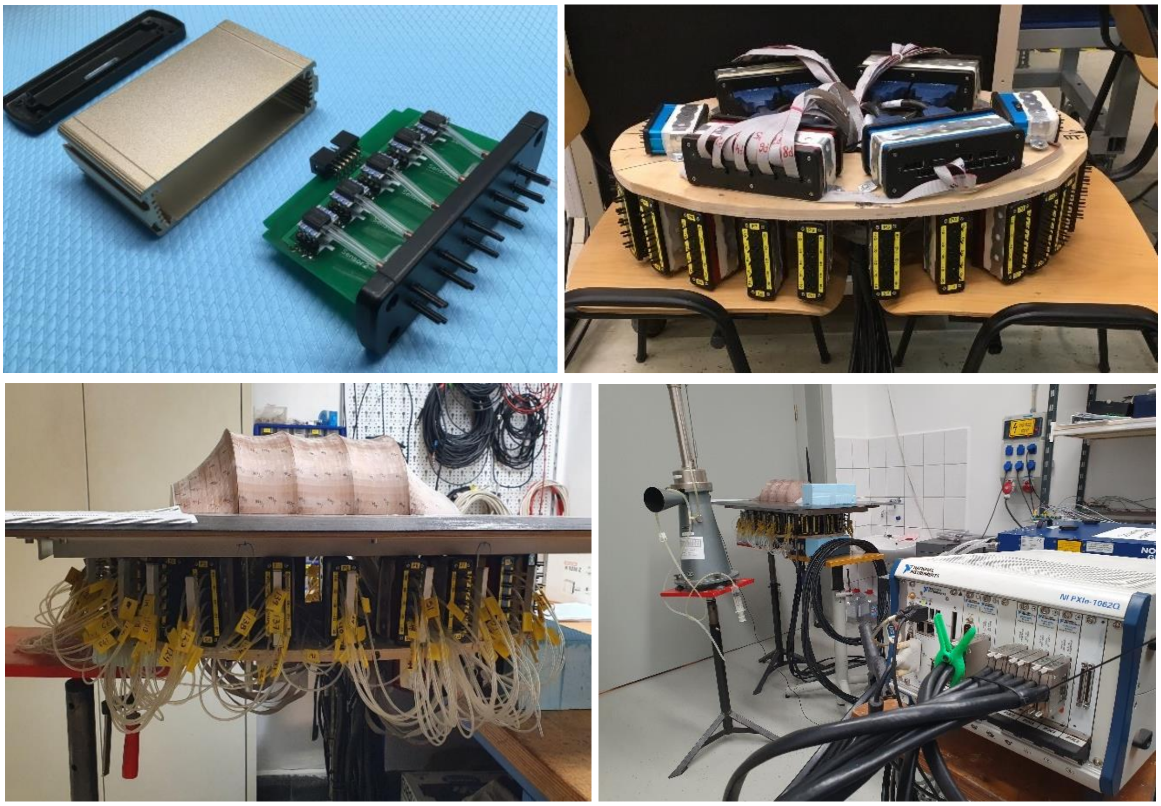

Figure 4. Top left: A satellite module of the multi-channel pressure measurement system. Top right: Assembly of satellite modules and signal distribution boxes. Bottom left: satellite modules installed underneath and connected to a wind tunnel model. Bottom right: connection to the NI PXI data acquisition system.

5.2 Outcome

A 400-channel simultaneous pressure measurement system, applicable to determination of wind loading on a wide range of buildings. The system has been used already in five projects since its construction in 2019, four of which were joint projects with industrial partners.

5.3 Acknowledgement of contributors

- Balázs Istók PhD: design, component selection, and partially manufacturing the PCB boards, assembly and testing of the system.
- Márton Koren, MSc, PhD student: design and partially manufacturing the PCB boards, programming the NI LabVIEW based DAQ software, testing of the system.

6 Programming of the data analysis software for multi-channel pressure measurements

6.1 Description

For the post-processing of the raw data captured by the multi-channel pressure measurement system described in Chapter 5, I developed a software [12-13]. The data processing steps implemented in the software and its documentation pin down the post-processing procedure applied in our wind tunnel laboratory and serve as a guideline, how to transform the output from a model scale wind tunnel test into full-scale. The program was written in LabVIEW environment and is able:

1) to compensate timeseries for the distorting effect of finite length tubing between pressure taps and sensors (the transfer function of tubing is determined in advance on a dynamic calibration rig including a loudspeaker and a reference pressure sensor)
2) to scale the captured pressure timeseries in time and magnitude, to resample, filter, average (to get for example pressure coefficient or full scale pressure timeseries)
3) to reduce the timeseries: calculate mean, RMS, actual, 1 s or 3 s-wind gust extreme values, and predict extreme values (using extreme value analysis)
4) to interpolate pressure timeseries in space and time to a surface mesh of the model building. The interpolated timeseries' RMS and extreme values should be consistent to those of the source (measured) timeseries. This is ensured using a simply modified, RMS-preserving inverse-distance method.
5) to calculate the load effect function time-series (e.g. the total base bending moment), if the influence coefficients of the selected load are given into the program, and calculate average and peak values of these loads (e.g. the highest base bending moment). (See an explanation in **Figure 5.)**

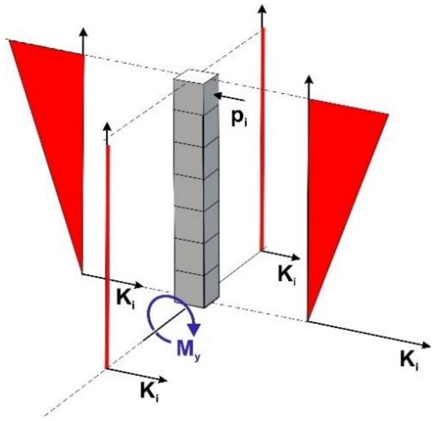

Figure 5. An explanation to load effect functions: The influence coefficients K_i (shown with red) assigned to the individual mesh elements let us determine the load function of the base moment of the building shown: $M_y(t) = \sum_{i=1}^{n} K_i \cdot p_i(t)$ with the pressure timeseries $p_i(t)$ in each cell centre i.

6) to determine peak values across many measured configurations and wind directions, thus calculate the overall peak loads of a structure.
7) to export reduced data programmatically in MS Excel sheets and time dependent pressure distributions into Tecplot 360 flow visualization software.

The program consists of 8300 nodes (~ equivalent to 8300 program lines in text-based programming languages) and 140 subroutines.

6.2 Outcome

The developed software allows the post-processing, export and communication of wind loads to the research parties in an internally standardized, documented way. Examples are shown in **Figure 6** and in a video **[14].**

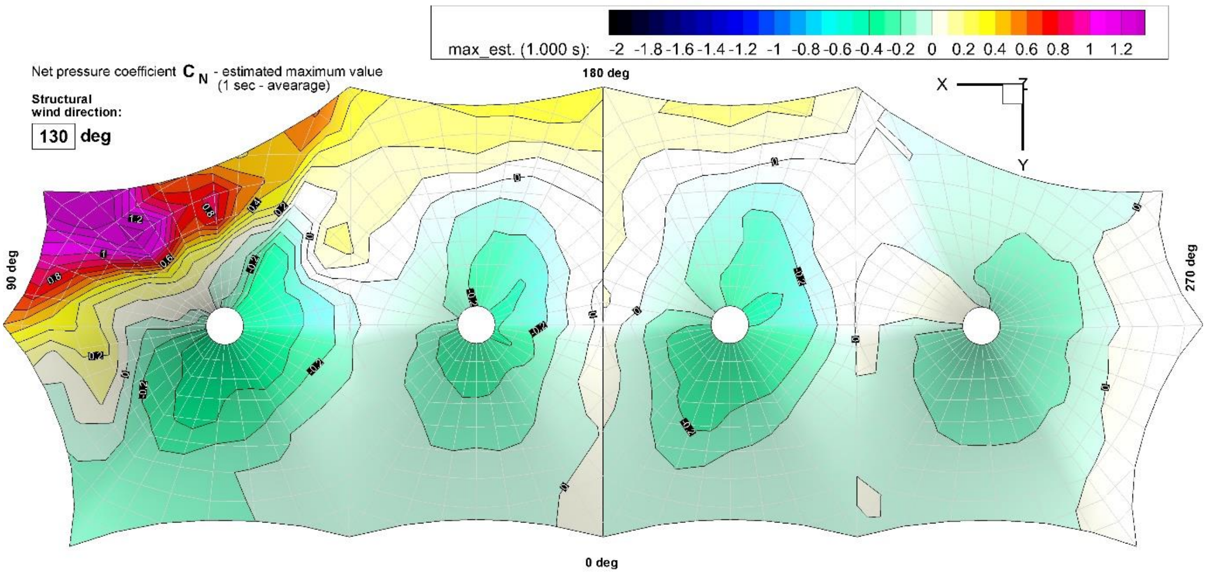

Figure 6: sample pressure distribution results: peak positive net pressure coefficient value on a tensioned fabric roof structure

6.3 Acknowledgement of contributors

Jenő M. Suda PhD, Balázs Farkas PhD, Márton Koren MSc: wind tunnel tests and acquisition of raw measurement data shown in Figure 6 and in [12]

6.4 References

[12] ARA Multi-channel Pressure Magic: Program help *(in Hungarian)* https://simba.ara.bme.hu/~balczo/out/K127919/12_ARA_MCP_Help.pdf

[13] ARA Multi-channel Pressure Magic: Program help videos *(in Hungarian)*: https://youtube.com/playlist?list=PLfclthpMe8UKyMeGwDGTvWTpYGKFbZa7x

[14] Video showing full scale pressure fluctuations on a tensioned fabric roof structure measured in wind tunnel, calculated by the program and exported by Tecplot 360: https://youtu.be/Tt4CXAqFIdU

7 Programming of a wind tunnel measurement control and data acquisiton program

7.1 Description

While recording laboratory procedures and best practices into internal guidelines seems the obvious choice to do to ensure the quality of operation the wind tunnel lab see e.g. [15], these need to be implemented into practice further. The best way to do is to anchor these into operational software(s). For this purpose, a LabVIEW-based general measurement control and data acquisition software bundle was developed by me since 2005.

The program ARA Pressure & Force is able to perform measurements of analogue sensors used in the lab (pressure transducers, load cells, CTA sensors), calibrate these statically, dynamically (determine the response function of pressure transducers and tubing) perform matrix calibration of multi axis force measurement systems, and is able to control multiple stepper motors and traversing systems of the company ISEL used in the lab, furthermore digital cameras, mechanical scanning valves, mass flow controllers and some of our wind tunnels themselves. The software has a graphical user interface and can run scripts in a primitive scripting language. The program consists of 14600 nodes and has 228 subroutines. The menu system shown in **Table 6** is informative about the available functions.

Table 6. Menu system of ARA Pressure & Force

File	New measurement | Open measurement | Save measurement as | Exit
Settings	Barometric pressure & temperature | Customize measurement table | Notification settings | Show measurement progress bar | Show advanced tab | Filter settings
Calibration	Linear transducer calibration | 1-D hotwire calibration | Multi-component balance calibration | Dynamic response calibration | Zero transducers
Devices	Traverse manager | Wind tunnel control | Scanivalve options | Scanivalve monitor | Camera setup | Brooks DMFC
Tools	Open postprocessing app | Update time-resolved data paths | Convert time-resolved data
Help	Help | Show help in English | Version changes | About

In the current PD project, the Large Wind Tunnel Traversing System (LWTTS) with a National Instruments NI 7344-based stepper controller has been integrated into this software bundle, allowing automated measurements through many measurement positions in the wind tunnel test section. (Before that, measurement could only be run in a separate software.)

One of the developed subroutines generates and previews the movement track, and helps to avoid hitting obstacles like the wind tunnel model. Measurement results, e.g. flow velocity measured with CTA can be visualized instantaneously after the measurement.

Another step towards standardizing lab procedures is the automatic generation of transducer calibration reports in PDF format. An example is shown in [14].

7.2 Outcome

The laboratory's basic measurement software ARA Pressure & Force (v. 4.52 as of January 2023) is able to perform measurements along tracked moves of the Large Wind Tunnel traversing system. The pre capability has been used during pollutant dispersion measurements of the boundary layer described in Chapter 8 for traversing of Pitot-static and CTA probes, and in project 'B' (traversing of the fast FID sampler).

To improve measurement documentation, calibration protocols are generated automatically. Further development of the software bundle is continuous.

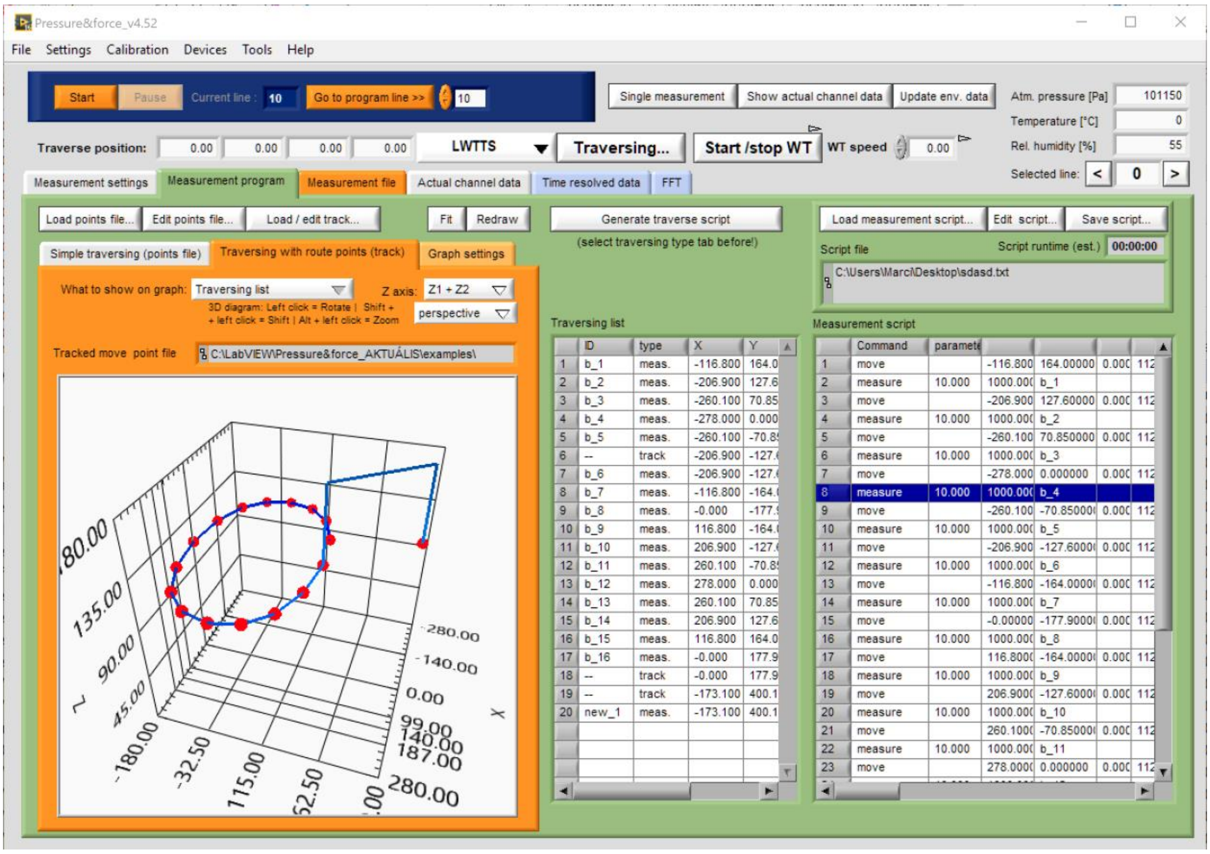

Figure 6: Graphical interface showing the integration of the LWTTS into the software: a measurement track on the left, and a script on the right.

7.3 Acknowledgement of contributors

PhD students Árpád Varga, MSc and Márton Koren MSc: programming of some subroutines for earlier versions of the software bundle.

7.4 References

[15] Balczó Márton (2019): Wind tunnel testing methods applied at the Theodore von Kármán Wind Tunnel Laboratory for determination of wind loading on buildings and structures. Brochure for wind tunnel users/clients. https://simba.ara.bme.hu/~balczo/out/K127919/15_KWTL_wind_tunnel_methods_2019.pdf

[16] Sample automatic calibration protocol of a pressure transducer, 9 March, 2021 https://simba.ara.bme.hu/~balczo/out/K127919/16_Sample_calibration_report_210309.pdf

[17] Video showing a remotely controlled wind tunnel measurement: https://youtu.be/_2RFzIbBxCk

8 Generation of atmospheric boundary layers in the wind tunnel

8.1 Description

In my original research plan, atmospheric boundary layer (BL) generation in a new boundary-layer wind tunnel with a corresponding long flow preparation section was envisaged. As the developments in project ‘A’ did not allow building a new one, we were limited to the existing closed return, open-test section wind tunnel, with its main disadvantage, a short test section of only some 3 m. Despite of this fact we tried and succeeded generating boundary layers.

First we used the traditional approach using vertical spires (vortex generators, a ground mounted fence and floor roughness elements) as described by [18, 19] at the inflow of the test section. In this case, we found that wind velocity was decreasing in longitudinal direction (by about 20% along the 2m-diemeter wind tunnel turntable), and lateral homogeneity was also as much as 10% within the central 1 m of the wind tunnel cross section, in spite of our several trials rearranging the distance between spires. The height of this BL was only about 400 mm.

As a second approach, to improve lateral homogeneity, we used horizontal bars of variable width placed at the inflow of the test section. While the method itself, already applied by [ref]. is not new, and was especially found useful in short test section tunnels, to find the desired profile, we applied a fast GPU-based CFD code.

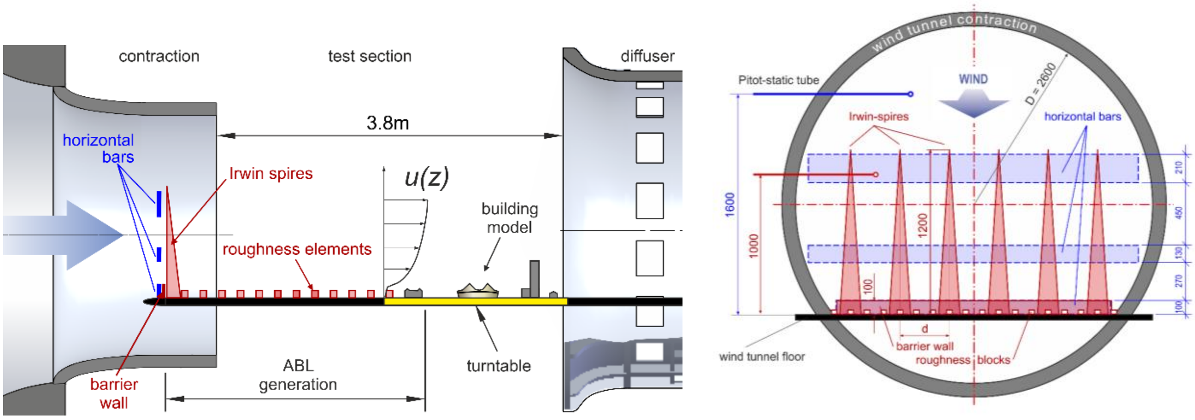

Figure 7: BL generation in the existing open test section wind tunnel using spires, barrier & roughness blocks (red); using horizontal bars (blue). Left: side view, right: front view. Dimensions in mm.

For CFD modeling, we used the GPU-based simulation software ANSYS Discovery Live 2019R3. transient flow simulations Navier-Stokes and continuity equations are solved in transient simulations using the Finite Volume Method (FVM) on an equidistant Cartesian mesh.. Turbulence is modelled using the standard Smagorinsky subgrid-scale stress model while the large-scale eddies are captured using LES.

The BL-generation procedure is as follows:

1. determine the mean and standard deviation of velocity in vertical direction for a given z_0 roughness length and model scale, and the necessary length scale of turbulent structures. (e.g. from EUROCODE, or ESDU [18-20])
2. Because turbulent length scales within the flow are closely related to the size of the vortex generators, size a couple of vortex generators based on required length scale distribution, and place them into a simulation model.
3. Start the GPU based CFD simulation with this initial setting.
4. While running the simulation, adjust gaps between the vortex generators and the size of the vortex generators in real time, on a trial and error basis to get a mean profile and turbulence level close to the desired one. Adjustment guidelines:
    a. more solidity (blocked cross sectional area/total cross sectional area) in the cross section: higher turbulence

b. more solidity close to the ground: decreasing wind velocity in the lower part of the profile
c. more horizontal bars of smaller size, smaller gaps: smaller turbulent length scale

This procedure has to be refined, mostly to replace the trial and error part with an optimization algorithm, however, even this method can reach the desired result in a couple of hours simulation, as shown in **Figure 9**. The lateral homogeneity has been improved compared to the first, traditional approach and a much deeper BL of ~800 mm could be generated, with a much better lateral and longitudinal homogeneity of less than 5% total deviation at within the central 1 x 1 m around the turntable centre. (**Figure 10**.)

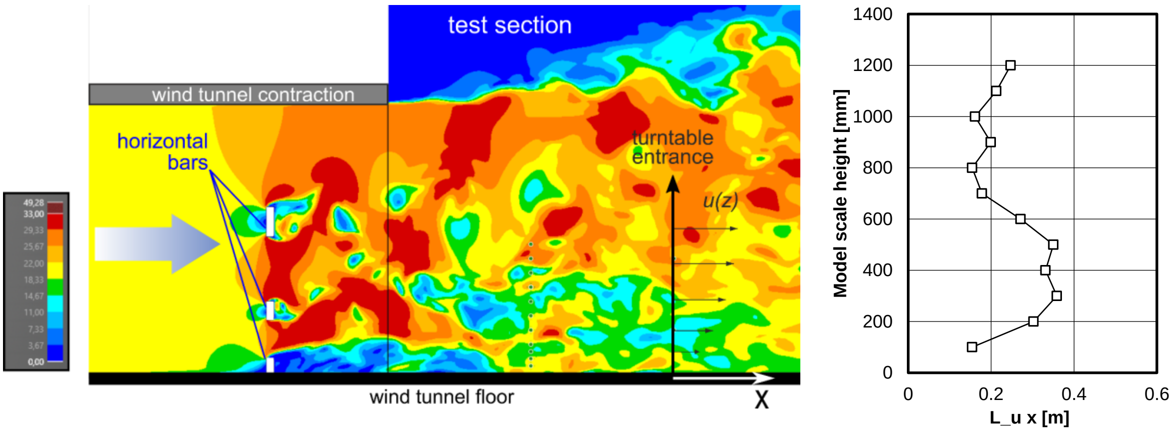

Figure 8: Longitudinal cross section of the simulation domain, and an instantaneous velocity distribution (velocity magnitude) showing flow structures in size correlated to the size of horizontal bars (inlet velocity at the entrance: 20 m/s) Right: measured turbulent length scale.

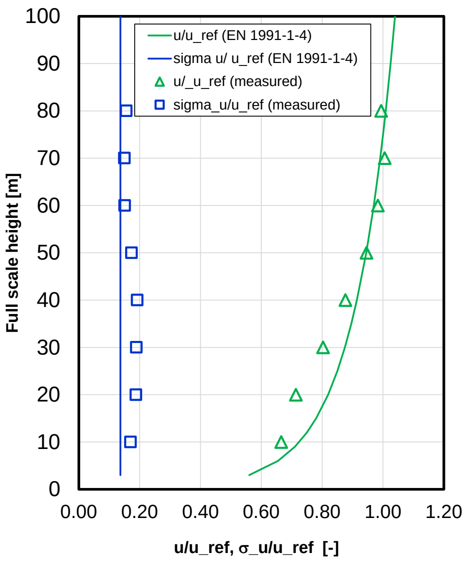

Figure 9. Boundary layer as required by EUROCODE for $z_0 = 0.05\ m$ (continuous line) and as set up in wind tunnel using GPU based CFD simulations and then measured by CTA. Reference height 80 m, model scale 1:100. Blue: green: mean velocity profile $\overline{u}/u_{ref}$, blue: relative standard deviation of velocity σ_u/u_{ref} .

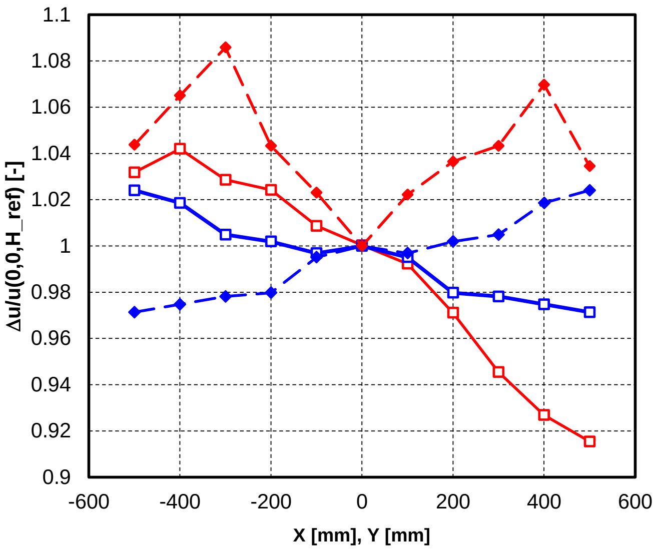

Figure 10. Comparison of BL homogeneity $\Delta\overline{u}/u_{ref}(0, 0, H_{ref})$ within the 1 x 1 m around the turn table centre. Dashed line: across test section (Y direction), continuous line: along the test section (X direction) Red: conventional method using spires, barrier wall & roughness blocks; blue: BL generated by horizontal bars.

8.2 Outcome

While the promised 4-5 different boundary layers have not been generated yet, we now have the promising arrangement and calculation method to generate BLs to the desired model scale and z_0 with sufficient height and lateral homogeneity.

8.3 Acknowledgement of contributors

- Bálint Papp, MSc, setting up and running ANSYS Discovery simulations
- Balázs Farkas PhD: running ANSYS Discovery simulations, building the second type BL generator elements
- Balázs Istók, PhD: building the second type BL generator elements
- Márton Koren MSc: Measurement of boundary layer in wind tunnel using CTA

8.4 References

[18] Counihan, J. (1973): Simulation of an adiabatic urban boundary layer in a wind tunnel. Atmospheric Environment (1967) 7 (7) 673-689. http://dx.doi.org/10.1016/0004-6981(73)90150-9

[19] Irwin, H. (1981): The design of spires for wind simulation. Journal of Wind Engineering and Industrial Aerodynamics 7 (3) 361-366. http://dx.doi.org/10.1016/0167-6105(81)90058-1

[20] NEN–EN 1991-1-4 (2005) Eurocode 1: Actions on structures - Part 1-4: General actions - Wind actions.

[21] ESDU (1972): ESDU 72026 Characteristics of wind speed in the lower layers of the atmosphere near the ground: strong winds (neutral atmosphere). Engineering Sciences Data Unit.

[22] ESDU (1974): ESDU 74031 Characteristics of atmospheric turbulence near the ground. Part II: single point data for strong winds (neutral atmosphere). Engineering Sciences Data Unit.

9 Test measurement of wind pressures on an arched roof structure

9.1 Description

Fabric roof structures, arched, tensioned or held by internal air pressure are widely used in architecture for spanning stadia, swimming pools, tennis courts, transport facilities, greenhouses etc. The custom shape requires wind tunnel tests, while wind load on roofshapes close to regular can be calculated using guidelines. Eurocode EN 1991-1-4 [18] gives e.g. pressure coefficients for arched (semi-cylindrical) structures. Underlying full scale and wind tunnel studies were published by [21-23].

The wind tunnel test presented here is a collaboration of myself and reasearchers of the BME Faculty of Civil Engineering, Department of Structural Mechanics. My job was assistance of the team in all aspects of wind tunnel testing, and running the tests themselves. The project will serve as a reference measurement of the wind tunnel, the boundary layer, the pressure measurement system as a whole, but also will provide additional data for their research, as the model will be tested at various wind directions and boundary layers.

The model is modular single span arched roof (see also **Figure 2**) with 3-5 bays, with hyperbolic surface, and semi-circular tensioning archs, thus represent a real-life tensioned structure. Arch height is H = 30 m, with arching of h/H = 0.93 between arches, an arch width B = 60 m, bay width L = 20 m. Model scale is 1:250, and the model is equipped with 180 pressure taps, in a 9 x 4 arrangement in each arch bay. At the current stage (December 2022) only measurement results in laminar, homogeneous flow for the 5-bay configuration are available. Further tests are still in progress. In **Figure 12** we show the pressure coefficient distribution, compared to earlier wind tunnel results (As the inflow conditions in this preliminary test were not equal, a full agreement of c_p values is not expected.)

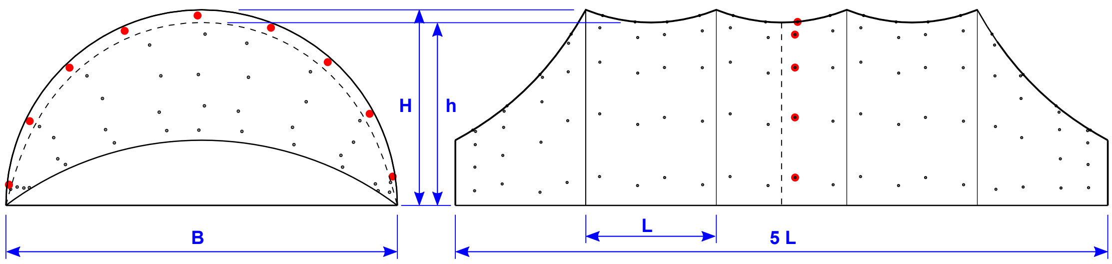

Figure 11: Geometry and pressure tap positions of the arched roof wind tunnel model, here with 3 bays. See also Figure 2. Symmetry axis pressure taps of the central bay indicated with red, all other tap locations by black dots.

9.2 Outcome

As mentioned in the Executive Summary, 2-year delay in the realization of project 'A' caused also this project part to slip, thus it is still underway. After performing tests at various number of bays, various wind directions and and various boundary layers, the results can be used to dimension arched roofs more precisely. Comparison to wind tunnel test results of [24] will demonstrate accuracy of our wind tunnel testing.

9.3 Acknowledgement of contributors

- Krisztián Hincz, PhD, associate professor (BME Faculty of Civil Engineering, Department of Structural Mechanics): Overall management of the research project, design of arched roof geometry, model preparation, structural calculations.
- Shirly Pool Blanco MSc, PhD student (BME Faculty of Civil Engineering, Department of Structural Mechanics): Arched roof model manufacturing, pressure tapping, preparation for measurement, accompanying CFD simulations

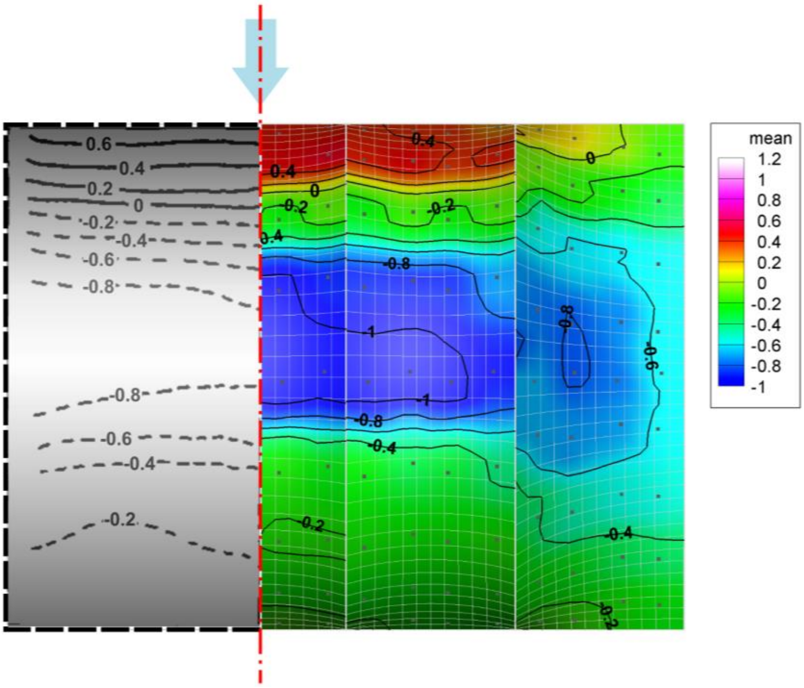

Figure 12: Comparison of mean pressure coefficient distribution at wind direction perpendicular to the long axis of the structure. As results are symmetrical to the wind axis, we only show one side of both datasets. On the left side we show literature data of a semicylindrical roof (L/H = 2) with vertical sidewalls in a BL flow [24]; on the right side: hyperbolical arched roof of the current investigation [Figure 11] in laminar flow.

9.4 References

[23] Cook, N.: Designer's Guide to Wind Loading of Building Structures Part 2: Static structures (Building Research Establishment Report), 1990.

[24] Toy, N. & Tahouri, B.: Pressure distributions on semi-cylindrical structures of different geometrical cross-sections. Journal of Wind Engineering and Industrial Aerodynamics, 1988, 29, 263-272 http://dx.doi.org/10.1016/0167-6105(88)90164-X

[25] Hoxey, R. P. & Richardson, G. M.: Measurements of wind loads on full-scale film plastic clad greenhouses. Journal of Wind Engineering and Industrial Aerodynamics, 1984, 16, 57-83 http://dx.doi.org/10.1016/0167-6105(84)90049-7

10 High-frequency force balance technique (HFFB) – replaced by low-frequency balance

10.1 Description

The significant modification of project ‘A’ did not allow the purchase of a High-frequency force balance (HFFB) transducer for budget reasons. This leaves the wind tunnel lab at the moment only with the High -Frequency Pressure Integration method, if extreme instantaneous wind loads of a structure has to be determined.

Low frequency balances (f_{limit} < 10 Hz) can be used however to determine the mean wind loads, and this might be satisfactory for simple structures. I developed a low-cost 3-component force balance which is implemented into the ARA Pressure&Force software, including the subroutine for matrix calibration with any DOF and order.

The force balance capabilities were demonstrated in the wind tunnel test of railway catenary masts, performed by the author, an excerpt of results is shown below in **Figure 13** and **14.** A repeatability and hysteresis error of $\Delta c_{D,T} = \pm 0.01$ and en extended overall error of $\Delta c_{D,T} = \pm 0.065$ has been reached for the total drag coefficients $c_{D,T}$ of mast models. ($c_{D,T}$ values ranged up to 2.5). A video is shown in [17].

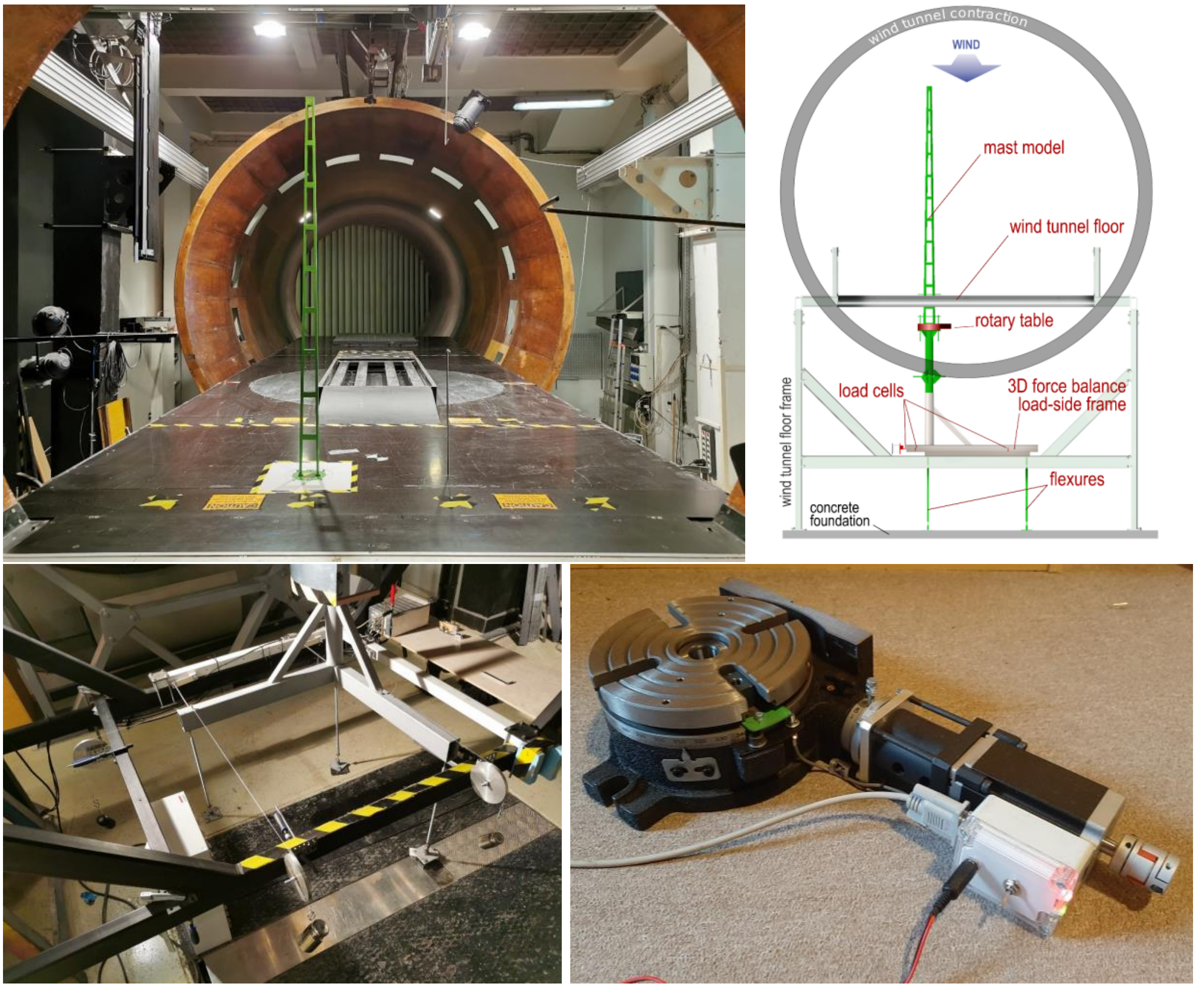

Figure 13. Top left: catenary mast wind tunnel test. Top right: measurement arrangement. Bottom left: calibration of the simple 3D force balance underneath the wind tunnel test section. Bottom right: Stepper driven rotary table built in.

10.2 Outcome

A simple 3-component low-frequency force balance system is available for the measurement of the drag force, side force, and torque around the vertical axis, including the necessary rotary table for model rotation, and integration into the laboratory software ARA Pressure&Force. It must be noted that this force balance is not suitable for the capture of time-dependent base forces and moments of a small-scale building or structure model, for which still a HFFB is required with f_{limit} > 100 Hz.

10.3 Acknowledgement of contributors

Bence Fenyvesi MSc, PhD student: assistance in model construction and wind tunnel testing of railway catenary masts.

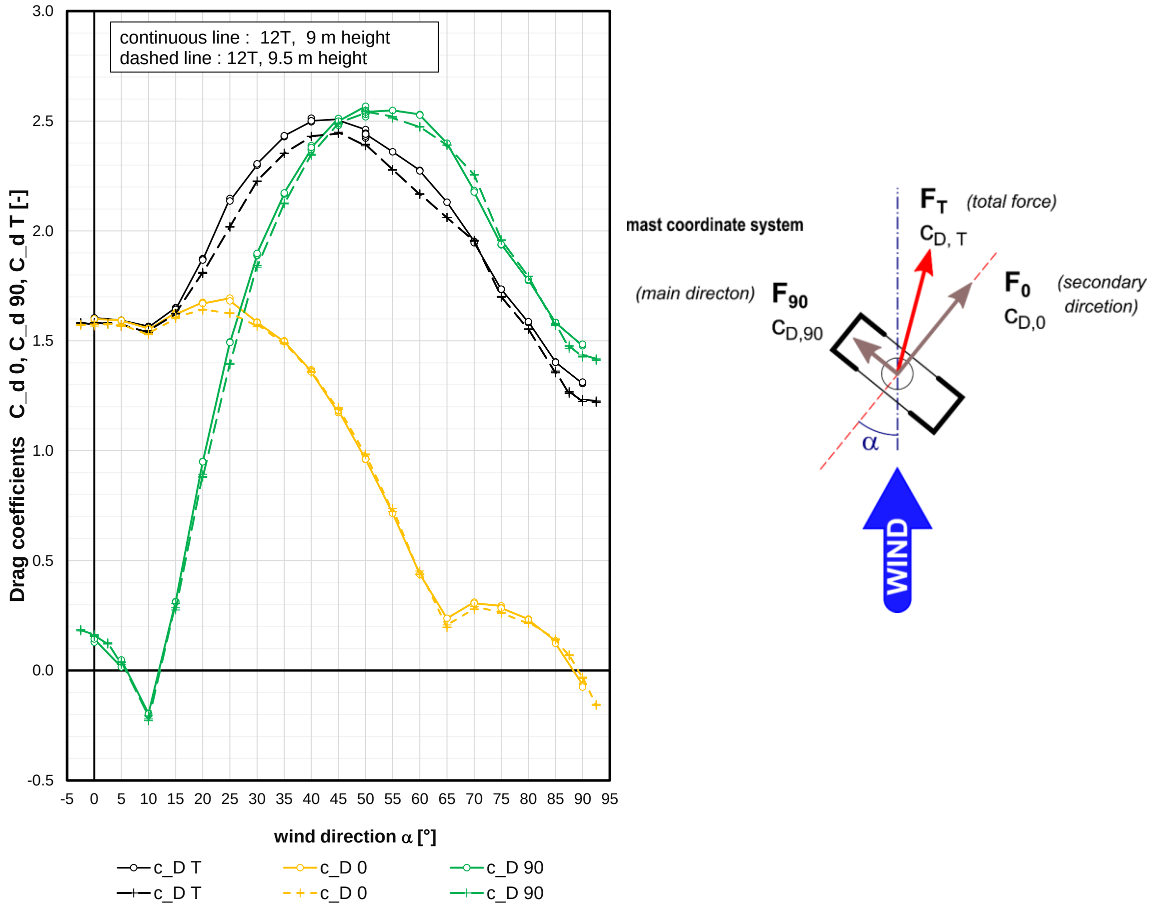

Figure 14. Sample measurement result from two, almost identical type T line catenary masts (Drag coefficient vs. wind direction). Right: definition of drag coefficients.

11 Appendix

1) Goldmann building laboratory design drawings
2) AE building design laboratory drawings
3) Model and prototype workshop
4) Pressure loss calculation of the closed return wind tunnel

GOLDMANN SZÉLCSATORNA ALAPRAJZI ELRENDEZÉS TERVEZET M =1:100
2019 . március 20. III . változat

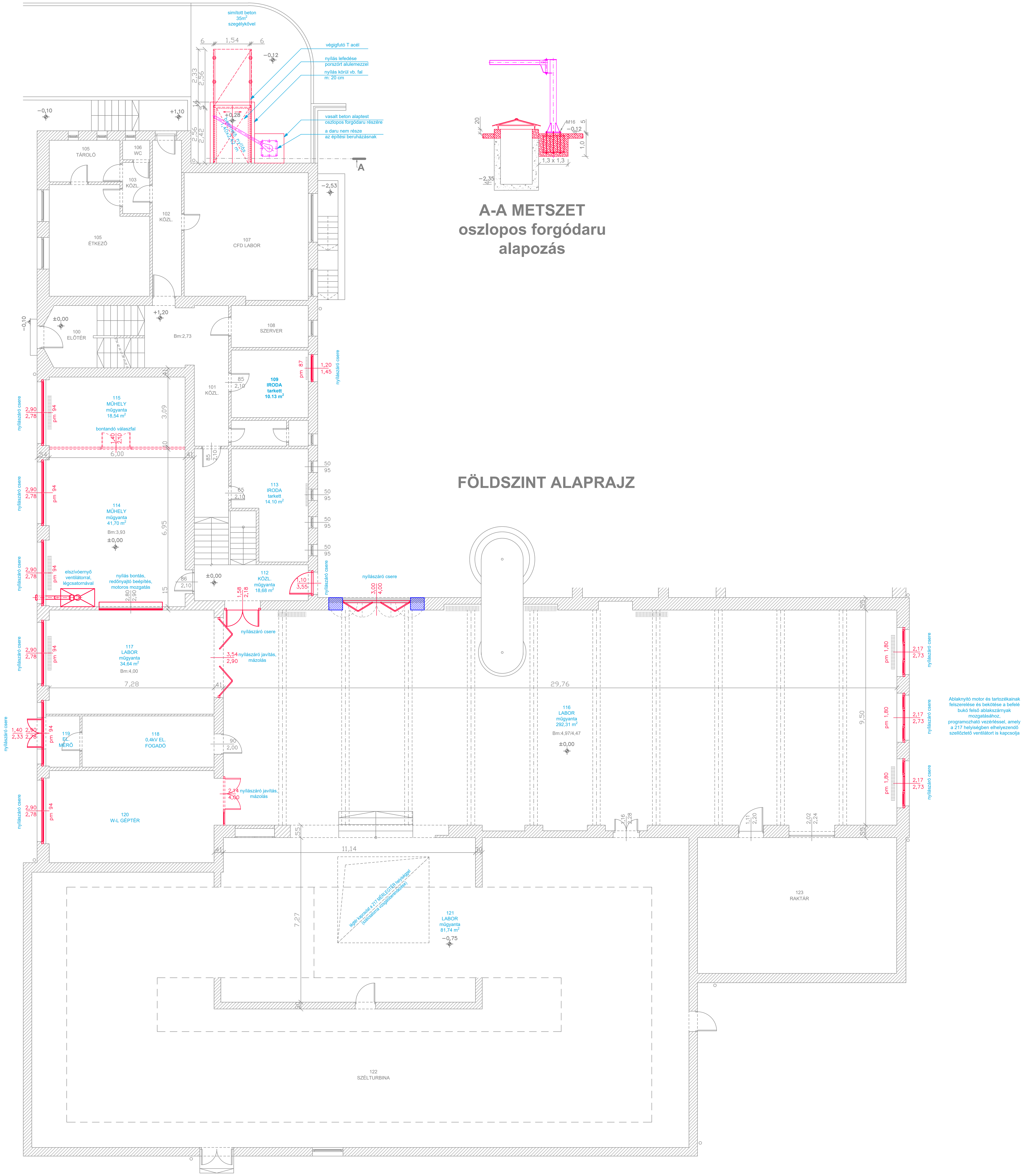

A-A METSZET
oszlopos forgódaru alapozás

FÖLDSZINT ALAPRAJZ

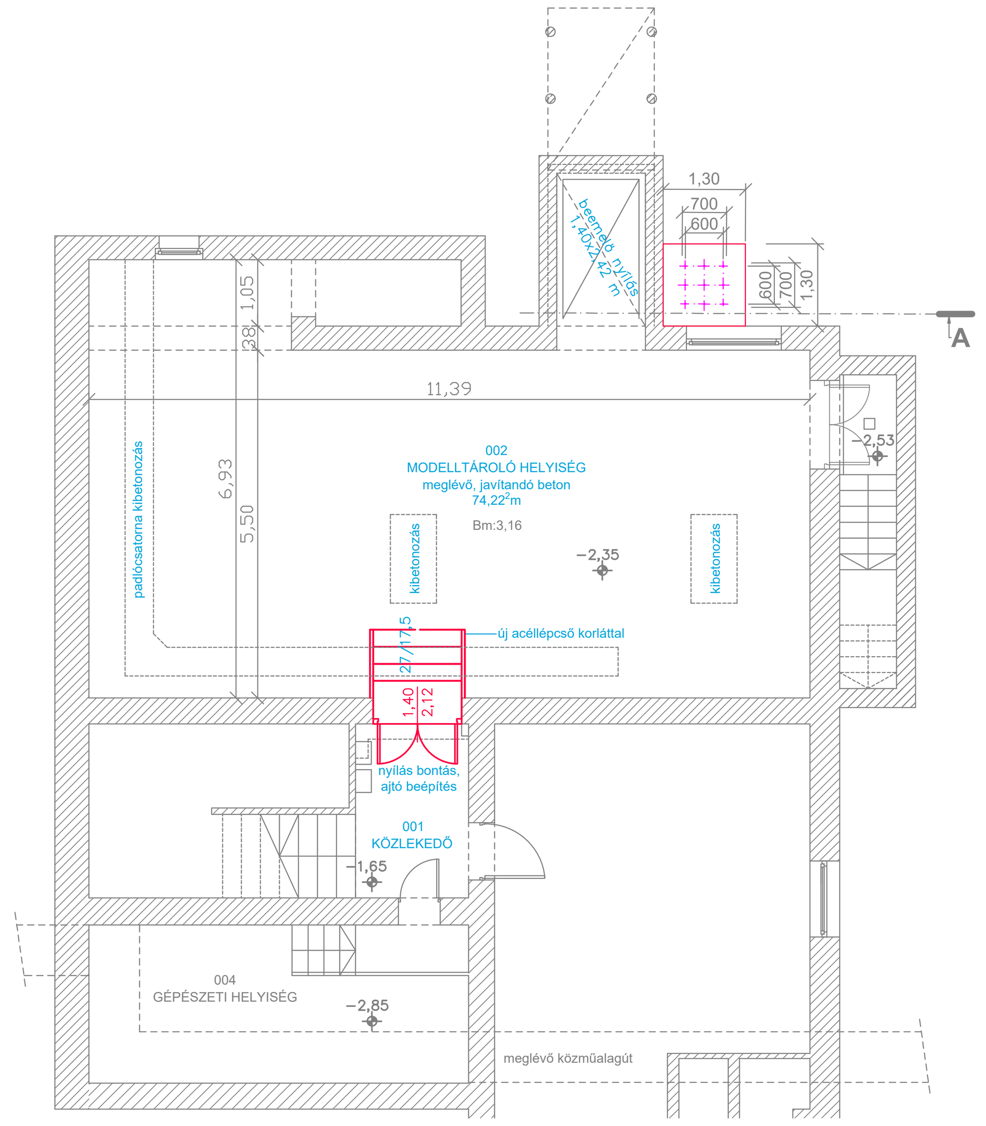

ALAGSOR ALAPRAJZ

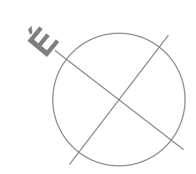

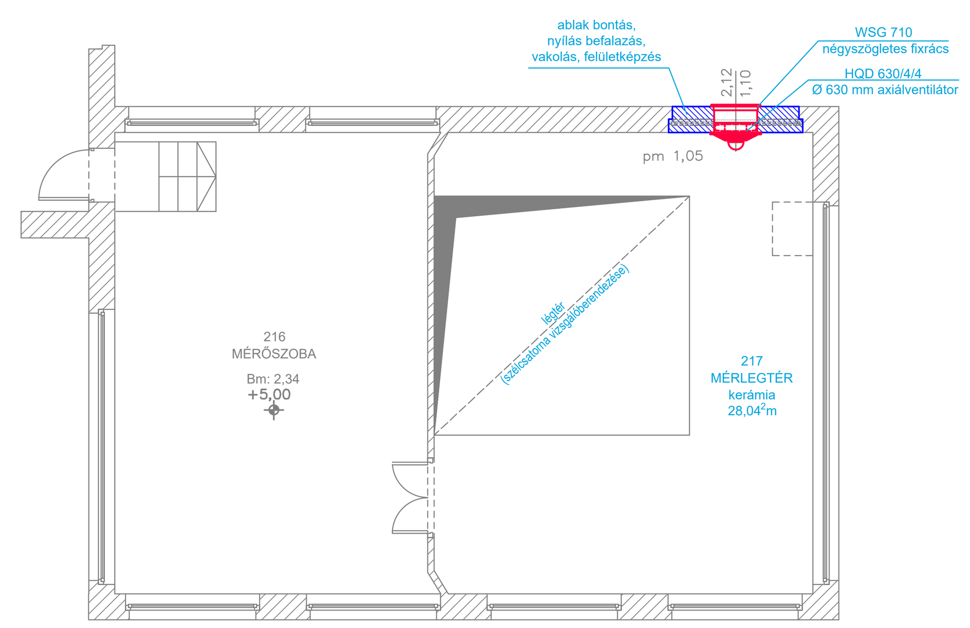

EMELT ALAPRAJZ

készítette:
Pálinkás József okl. gm.
épületgépész műszaki ellenőr

BUDAPESTI MŰSZAKI ÉS GAZDASÁGTUDOMÁNYI EGYETEM
Kancellária
Budapest, XI. ker. Műegyetem rkp. 3.

BME "AE" ÉPÜLET
Gépészmérnöki Kar Áramlástan Tanszék
ATMOSZFÉRIKUS ÁRAMLÁSOK LABORATÓRIUM KIALAKÍTÁSA
1111 Budapest, Bertalan Lajos u. 6. (Hrsz.: 4110)

ALAPRAJZ

DÁTUM:	LÉPTÉK:	RAJZSZÁM:
2019. 11. 17.	M = 1:100	**É-01**

Appendix 3 : **Model and prototyping workshop**

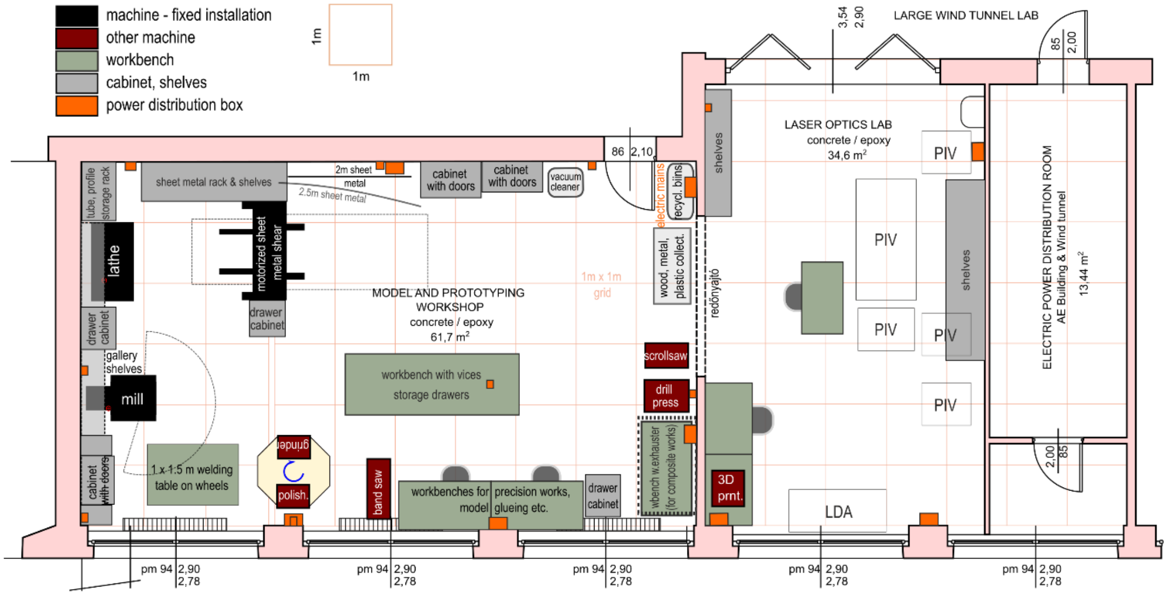

Workshop layout

The workshop as realized in summer 2022

Appendix 4: **Pressure loss calculation of the closed return wind tunnel**

No.	ID	Section name	Height at inlet	Width at inlet	Length	Half-angle	Area	Speed	p_din	ζ	η	Δp'	p_{stat_out}
		-	m	m	m	°	m2	m/s	Pa	-	-	Pa	Pa
		(Contraction outlet geom)	2.1	3.8			7.98	26.0					39
1	TS	Test section	2.1	3.8	18		7.98	26.0	399	**0.413**		165	13
2	BR	Breather	2.6	3.8	0.1		9.88	21.0	260	**0.05**		13	0
3	D1	Test section outlet diffuser	2.60	3.80	2	0	9.88	21.0	260		**0.75**	0	0
4	TV1	Turning vanes 1	2.60	3.80	3.80		9.88	21.0	260	**0.12**		31	-31
5	D2	Turning vane connection diffuser	2.60	3.80	3	1.3	9.88	21.0	260		**0.75**	15	13
6	TV2	Turning vanes 2	2.74	4.10	4.10		11.23	18.5	201	**0.12**		24	-11
7	D3	Before fan diffuser	2.74	4.10	2.95	3	11.23	18.5	201	**0.1**		20	-128
8		Before fan noise damper	3.05	4.41	3.6		9.24	22.5	298	0.04		12	-140
		Fan			0.6		9.24	22.5				-696	556
10		After fan noise damper & casing	0.00	0.00	3.6		9.24	22.5	298	0.04		12	701
11	D4	After fan diffuser	3.05	4.41	11	2	13.44	15.4	141		**0.75**	25	778
	H1	Heat exchanger	4.20	6.10	1		25.62	8.1	39	**3.5**		135	642
12	TV3	Turning vanes 3	4.20	6.10	6.10		25.62	8.1	39	**0.12**		5	638
13	TV4	Turning vanes 4	4.20	6.10	6.10		25.62	8.1	39	**0.12**		5	633
14	SCR1	Screen 1	4.20	6.10	0.30		25.62	8.1	39	**1.5**		58	575
15	HC1	Honeycomb 1	4.20	6.10	0.50		25.62	8.1	39	**0.8**		31	544
16	SCR2	Screen 2	4.20	6.10	0.30		25.62	8.1	39	**1.5**		58	486
17	SCR3	Screen 3	4.20	6.10	0.30		25.62	8.1	39	**1.5**		58	428
18	SCR4	Screen 4	4.20	6.10	0.30		25.62	8.1	39	**0**		0	428
19	C1	Contraction	4.20	6.10	3.76		25.62	8.1	39		**0.92**	29	39
		(Contraction outlet geom)	2.1	3.8			7.98	26.0					

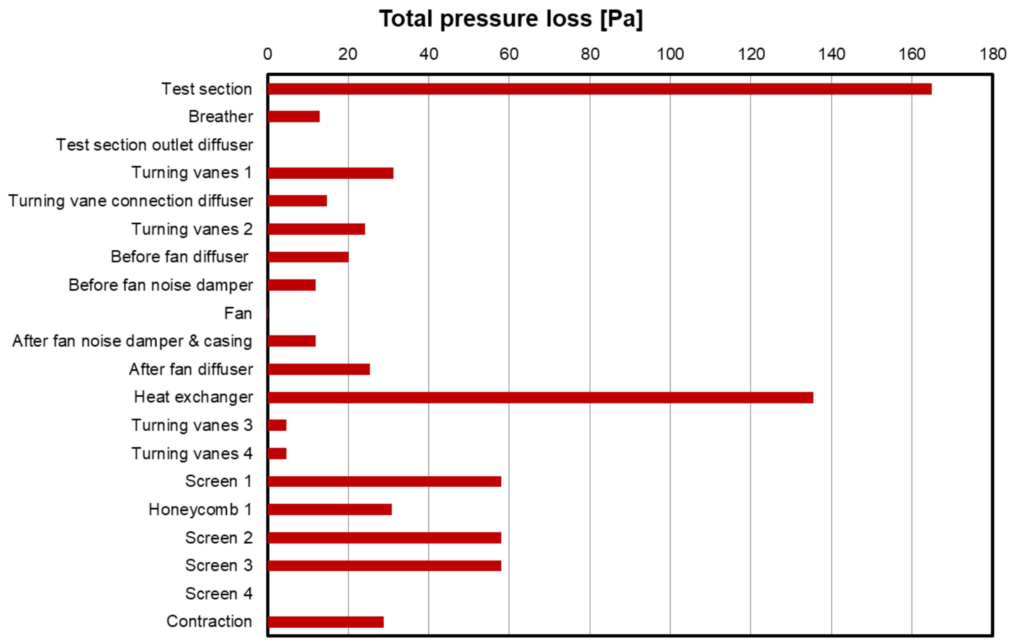

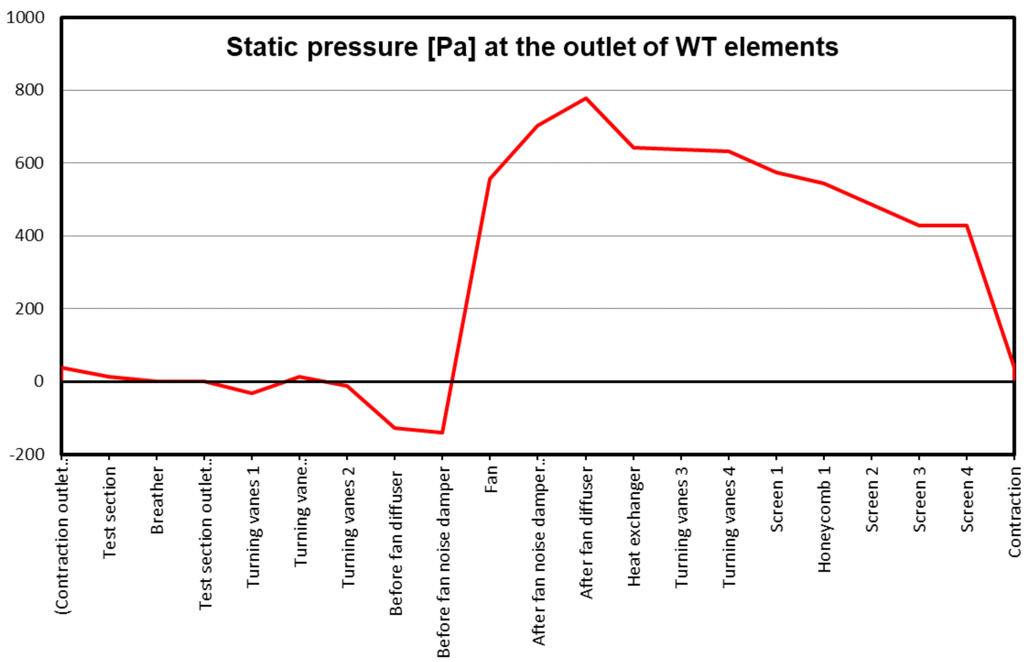

Price estimate of wind tunnel in autumn 2019

Subtask	**Estimated, million HUF**
Aerodynamic and acoustic design	3.2
Cooling system design	5.1
Structural design	14
Construction and installation of wind tunnel sections	96
Installation of cooling system elements	76.7
Fans	29
Electric works	7.6
Totalling	**231.6**